ELSEVIER

Astroparticle Physics 17 (2002) 205–220

Astroparticle Physics

www.elsevier.com/locate/astropart

A frequentist analysis of solar neutrino data

M.V. Garzelli *, C. Giunti

INFN, Sezione di Torino, Dipartimento di Fisica Teorica, Università di Torino, Via P. Giuria 1, I-10125 Torino, Italy

Received 25 October 2000; received in revised form 3 April 2001; accepted 31 May 2001

Abstract

We estimate with Monte Carlo the goodness of fit and the confidence level of the standard allowed regions for the neutrino oscillation parameters obtained from the fit of solar neutrino data. The Monte Carlo estimates are significantly smaller than the corresponding standard values. Using Neyman's method, we also calculate exact allowed regions with correct frequentist coverage assuming the standard least-squares estimator of the oscillation parameters. Our results show that the standard allowed region around the global minimum of the least-squares function is a reasonable approximation of the exact one, whereas the size of the other regions is underestimated in the standard method. © 2002 Elsevier Science B.V. All rights reserved.

1. Introduction

The standard method to analyze solar neutrino data in terms of neutrino oscillations consists in performing a least-squares fit. However, for the reasons described in Section 2 the standard least-squares analysis of solar neutrino data is approximate from a statistical point of view.

In this paper we present statistical methods based on Monte Carlo numerical calculations that allow to improve the implementation of the least-squares fit of solar neutrino data. In Section 2 we review the standard method and we discuss why its approximate assumptions could lead to significant inaccuracy in the results. In Section 3 we present a Monte Carlo method that allows to estimate the goodness of fit of solar neutrino data. In Section 4 we present a Monte Carlo method that allows to estimate the confidence level of the usual allowed regions in the space of the neutrino oscillation parameters. In Section 5 we present an implementation to solar neutrino analysis of the classical frequentist Neyman method that allows to calculate exact confidence regions with correct coverage.

Since the purpose of this paper is to illustrate different methods for the statistical analysis of solar neutrino data, we consider for simplicity only the data relative to the total rates measured in the Homestake [1] and Super-Kamiokande [2] experiments, and the weighted average of the total rates measured in the two gallium experiments GALLEX [3] and SAGE [4]. The values of these rates are given in Table 1 of Ref. [5]. Updated results of the Super-Kamiokande experiments and first results of the new GNO experiments have been presented in the recent Neutrino 2000 conference [6]. Since the numerical calculations presented here take a long time and were started before the Neutrino 2000 conference, we do not take into

* Corresponding author. Tel.: +39-11-6707241.
E-mail address: giunti@to.infn.it (C. Giunti).

0927-6505/02/$ - see front matter
PII: S0927-6505(01)00151-7

account the new data. A complete analysis including the new data and the Super-Kamiokande data relative to the electron energy spectrum and the zenith-angle distribution is under way and will be published elsewhere [7].

Neutrino oscillations[1] depend on the mass-squared difference $\Delta m^2 \equiv m_2^2 - m_1^2$ and on the mixing angle θ, that is restricted in the interval $[0, \pi/2]$. Traditionally solar neutrino data have been analyzed in terms of the parameters Δm^2 and $\sin^2 2\theta$, that determine the probability of neutrino oscillations in vacuum. However, it has recently been shown that the parameter $\tan^2\theta$ is more convenient for finding the allowed regions in the interval $\pi/4 \leqslant \theta \leqslant \pi/2$ when matter effects are important [10,11].[2] Moreover, the parameter $\tan^2\theta$ allows a better view of the regions at large mixing angles with respect to the usual parameters $\sin^2 2\theta$. Hence, in the following we analyze the solar neutrino data in terms of the parameters Δm^2 and $\tan^2\theta$.

Our calculation of the theoretical event rates follows the standard method described in several papers for matter-enhanced MSW [16] transitions [17–19] and vacuum oscillations [19,20]. We calculate the MSW survival probability of ν_e's in the Sun using the standard analytic prescription [9,17,18,21] and the level-crossing probability appropriate for an exponential density profile [17,22]. We calculate the regeneration in the Earth using a two-step model of the Earth density profile [23–27], that is known to produce results that do not differ appreciably from those obtained with the correct density profile. We have used the tables of neutrino fluxes, solar density and radiochemical detector cross-sections available in Bahcall's web page [28]. For simplicity we have neglected the matter effects that slightly affect the vacuum oscillation solutions of the solar neutrino problem, as discussed in Refs. [29,30].

2. Standard statistical analysis

The traditional way to find the values of the neutrino oscillation parameters Δm^2, $\tan^2\theta$ allowed by solar neutrino data is to perform a least-squares fit, often called "χ^2 fit". In this method the estimates of the parameters Δm^2, $\tan^2\theta$ are obtained by minimizing the least-squares function

$$X^2 = \sum_{j_1,j_2} \left(R_{j_1}^{(\mathrm{thr})} - R_{j_1}^{(\mathrm{exp})}\right)(V^{-1})_{j_1 j_2}\left(R_{j_2}^{(\mathrm{thr})} - R_{j2}^{(\mathrm{exp})}\right), \tag{1}$$

where V is the covariance matrix of experimental and theoretical uncertainties, $R_j^{(\mathrm{exp})}$ is the event rate measured in the jth experiment and $R_j^{(\mathrm{thr})}$ is the corresponding theoretical event rate, that depends on Δm^2 and $\tan^2\theta$.

The standard method for the calculation of the covariance matrix V is the one presented in Refs. [31,32], in which the independent uncertainties σ_j^2 of the experimental rates $R_j^{(\mathrm{exp})}$, and the uncertainties of the theoretical rates $R_j^{(\mathrm{thr})}$ are added in quadrature. Here we use this method, with the only difference that we assume a complete correlation of the errors of the averaged cross-sections for the fluxes in each experiment [33]. Since these correlations are not known, the choice of complete correlations is the safest approach. Hence, using the notation of Refs. [31,32],[3] the covariance matrix V is given by

$$V_{j_1 j_2} = \delta_{j_1 j_2}\sigma_{j_1}^2 + \delta_{j_1 j_2}\left(\sum_{i_1} R_{i_1 j_1}^{(\mathrm{thr})}\Delta \ln C_{i_1 j_1}^{(\mathrm{thr})}\right)^2 + \sum_{i_1,i_2} R_{i_1 j_1}^{(\mathrm{thr})} R_{i_2 j_2}^{(\mathrm{thr})} \sum_k \alpha_{i_1 k}\alpha_{i_2 k}(\Delta \ln X_k)^2, \tag{2}$$

where

$$R_{ij}^{(\mathrm{thr})} = \phi_i^{\mathrm{SSM}} C_{ij}^{(\mathrm{thr})} \tag{3}$$

is the event rate in the jth experiment due to the neutrino flux ϕ_i^{SSM} produced in the ith thermonu-

[1] Here we consider the minimal two-neutrino model, although more complicated models are possible (see Refs. [8,9]).

[2] For the same reason the parameter $\tan^2\theta$ has been employed in the framework of three-neutrino mixing [12–14] and the parameter $\sin^2\theta$ has been employed in the framework of four-neutrino mixing [15].

[3] The indices $j, j_1, j_2 = 1, 2, 3$ indicate the three solar neutrino experiments GALLEX + SAGE [3,4], Homestake [1] and Super-Kamiokande [2], respectively. The indices $i, i_1, i_2 = 1, \ldots, 8$ denote the solar neutrino fluxes produced in the eight solar thermonuclear reactions *pp*, *pep*, H*ep*, Be, B, N, O, F, respectively. The index $k = 1, \ldots, 11$ indicate the eleven input astrophysical parameters in the SSM (see Refs. [31,32]).

clear reaction in the Sun according to the SSM and $C_{ij}^{(\mathrm{thr})}$ is the corresponding energy-averaged cross-section that depends on Δm^2 and $\tan^2\theta$. The quantity $\Delta \ln C_{ij}^{(\mathrm{thr})} = \Delta C_{ij}^{(\mathrm{thr})}/C_{ij}^{(\mathrm{thr})}$ is the relative uncertainly of the energy-averaged cross-section $C_{ij}^{(\mathrm{thr})}$, that is taken to be approximately equal to the one calculated without neutrino oscillations.

The quantities X_k are the input astrophysical parameters in the SSM, whose relative uncertainties $\Delta \ln X_k$ determine the correlated uncertainties of the neutrino fluxes ϕ_i^{SSM} through the logarithmic derivatives

$$\alpha_{ik} = \frac{\partial \ln \phi_i^{\mathrm{SSM}}}{\partial \ln X_k}. \tag{4}$$

The values of $\Delta \ln C_{ij}^{(\mathrm{thr})}$, α_{ik}, $\Delta \ln X_k$ are given in Ref. [32].

Notice that, since the theoretical rates $R_{ij}^{(\mathrm{thr})}$ depend on Δm^2 and $\tan^2\theta$, also the covariance matrix V depends on Δm^2 and $\tan^2\theta$.

In the traditional method the observed minimum $(X^2_{\mathrm{min}})_{\mathrm{obs}}$ of the least-squares function (1) provides the estimate of the neutrino oscillation parameters, usually called "best-fit values". The goodness of the fit is estimated by calculating the probability to observe a minimum of X^2 larger than the one actually observed assuming for X^2_{min} a χ^2 distribution with $N_{\mathrm{exp}} - N_{\mathrm{par}} = 1$ degrees of freedom, where $N_{\mathrm{exp}} = 3$ is the number of experimental data points (the sums over j_1 and j_2 in Eq. (1) are from 1 to N_{exp}) and $N_{\mathrm{par}} = 2$ is the number of fitted parameters. Calling α this probability, one says that the fit is acceptable at $100\alpha\%$ CL. If α is larger than a minimum acceptable value, usually $\sim 10^{-2}$, the fit is considered to be acceptable and one can proceed further to determine the uncertainties in the determination of the parameters Δm^2 and $\tan^2\theta$ (the allowed regions in parameter space).

The standard regions of the parameters $\tan^2\theta$, Δm^2 allowed at $100\beta\%$ CL are those that satisfy the condition

$$(X)^2_{\mathrm{obs}}(\tan^2\theta, \Delta m^2) \leqslant (X^2_{\mathrm{min}})_{\mathrm{obs}} + \Delta X^2(\beta), \tag{5}$$

where $(X^2)_{\mathrm{obs}}$ are the observed values of X^2 as a function of the neutrino oscillation parameters and $\Delta X^2(\beta)$ is such that the probability to find $\chi^2 < \Delta X^2(\beta)$ is equal to β, in the case of a χ^2 distribution with $N_{\mathrm{par}} = 2$ degrees of freedom (the number of parameters). Common values for β are 0.90 (1.64σ), 0.95 (1.96σ), 0.99 (2.58σ), 0.9973 (3.00σ), 0.9995 (3.50σ), which give $\Delta X^2(0.90) = 4.61$, $\Delta X^2(0.95) = 5.99$, $\Delta X^2(0.99) = 9.21$, $\Delta X^2 \times (0.9973) = 11.83$, $\Delta X^2(0.9995) = 15.35$. The corresponding allowed regions in the $\overline{\mathrm{MSW}}$ area

$$10^{-4} \leqslant \tan^2\theta \leqslant 2, \quad 10^{-8} \leqslant \Delta m^2 \leqslant 10^{-3}\ \mathrm{eV}^2 \quad (\overline{\mathrm{MSW}}\ \mathrm{area}), \tag{6}$$

where matter effects are important [16], are shown in Fig. 1 and those in the $\overline{\mathrm{VO}}$ area

$$0.1 \leqslant \tan^2\theta \leqslant 1, \quad 10^{-11} \leqslant \Delta m^2 \leqslant 10^{-8}\ \mathrm{eV}^2 \quad (\overline{\mathrm{VO}}\ \mathrm{area}), \tag{7}$$

where vacuum oscillations are dominant, are shown in Fig. 2. The standard classification of the allowed regions is [4] (see Refs. [5,37]): SMA for

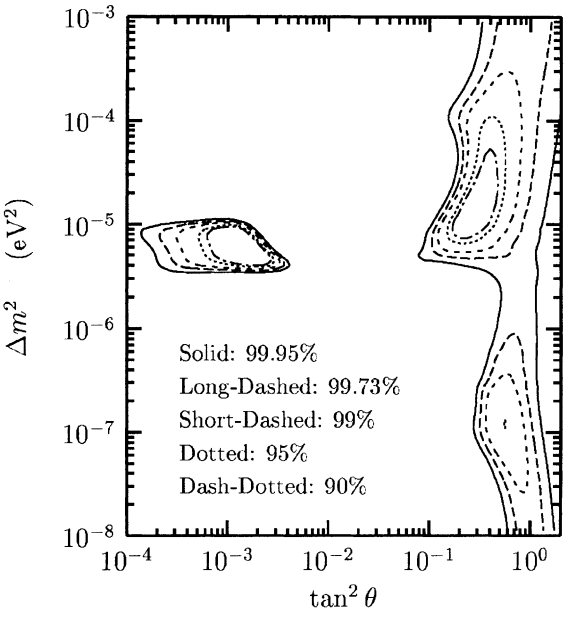

Fig. 1. Standard 90% (1.6σ), 95% (2σ), 99% (2.6σ), 99.73% (3σ), and 99.95% (3.5σ) CL allowed regions in the $\overline{\mathrm{MSW}}$ area (6).

[4] In this paper we use the standard names (SMA, LMA, LOW, VO) for the allowed regions at some confidence level, and we denote by $\overline{\mathrm{MSW}}$, $\overline{\mathrm{VO}}$, $\overline{\mathrm{SMA}}$, $\overline{\mathrm{LMA}}$, $\overline{\mathrm{LOW}}$ the rectangular areas in the $\tan^2\theta$–Δm^2 defined, respectively, in Eqs. (6), (7), (11), (12) and (13).

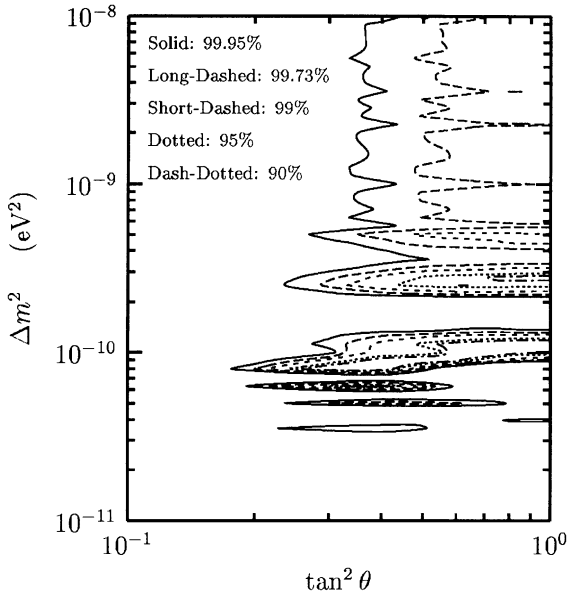

Fig. 2. Standard 90% (1.6σ), 95% (2σ), 99% (2.6σ), 99.73% (3σ), and 99.95% (3.5σ) CL allowed regions in the $\overline{\text{VO}}$ area (7).

$\Delta m^2 \sim 5 \times 10^{-6}$ eV^2, $\tan^2\theta \sim 10^{-3}$, LMA for $\Delta m^2 \sim 3 \times 10^{-5}$ eV^2, $\tan^2\theta \sim 0.3$, LOW for $\Delta m^2 \sim 10^{-7}$ eV^2, $\tan^2\theta \sim 0.5$, VO for $\Delta m^2 \lesssim 10^{-8}$ eV^2.

The standard procedure for the analysis of solar neutrino data would be correct if the theoretical rates $R_j^{(\text{thr})}$ depended *linearly* on the parameters Δm^2 and $\tan^2\theta$ to be determined in the fit and the errors $R_j^{(\text{thr})} - R_j^{(\text{exp})}$ were *multinormally* distributed with *constant* covariance matrix V. Indeed, if these requirements were realized one could prove that X^2 has a χ^2 distribution with $N_{\text{exp}} = 3$ degrees of freedom, X^2_{min} has a χ^2 distribution with $N_{\text{exp}} - N_{\text{par}} = 1$ degrees of freedom, and $X^2 - X^2_{\text{min}}$ has a χ^2 distribution with $N_{\text{par}} = 2$ degrees of freedom (see Refs. [34–36]). In this case the X^2 function would depend quadratically on the parameters and there would be only one allowed region with ellipsoidal form in the space of the parameters Δm^2 and $\tan^2\theta$.

In the case of solar neutrino data the gaussian distribution of experimental and theoretical uncertainties seems to be widely accepted, although it is not clear if this assumption is appropriate for the theoretical errors. On the other hand it is clear that

1. The theoretical rates $R_j^{(\text{thr})}$ do not depend at all linearly on the parameters Δm^2, $\tan^2\theta$. This is the reason why there are several allowed regions in the $\tan^2\theta$–Δm^2 plane (or the more traditional $\sin^2 2\theta$–Δm^2 plane) and the main reason why the allowed regions do not have elliptic form (see Refs. [5,37]).
2. The covariance matrix V is not constant, but depends on Δm^2 and $\tan^2\theta$, as remarked after Eq. (4). This fact contributes to the distortion of the allowed regions with respect to the elliptic form.
3. The errors $R_j^{(\text{thr})} - R_j^{(\text{exp})}$ are not multinormally distributed, because although the fluxes ϕ_i^{SSM} and the cross-sections $C_{ij}^{(\text{thr})}$ are assumed to be multinormally distributed, their products (3), that determine the theoretical rates through the relations

$$R_j^{(\text{thr})} = \sum_i R_{ij}^{(\text{thr})}, \tag{8}$$

are not multinormally distributed (see Ref. [38]).

Hence, the usual method of calculating the goodness of fit and the allowed regions in the $\tan^2\theta$–Δm^2 plane is not guaranteed to give correct results, i.e. the goodness of fit could be significantly different from $100\alpha\%$ and the confidence level of the regions obtained with the prescription (5) could be significantly different from $100\beta\%$.

We believe that the largest correction is due to the non-linear dependence of the theoretical rates $R_j^{(\text{thr})}$ from the parameters Δm^2, $\tan^2\theta$, that causes the existence of more than one local minima of the least-squares function X^2. This implies that there are more possibilities to obtain good fits of the data and the true goodness of fit is likely to be smaller than $100\alpha\%$. Also, in repeated experiments the global minimum has significant chances to occur far from the true (unknown) value of the parameters Δm^2, $\tan^2\theta$, leading to a smaller probability that the allowed regions cover the true value with respect to the linear case. Hence, we expect that the true confidence level of a usual $100\beta\%$ CL allowed region is smaller than β.

In the following sections of this paper we perform a least-squares fit of the solar neutrino data using the standard X^2_{min} estimator for the neutrino

oscillation parameters Δm^2, $\tan^2\theta$. We assume the usual gaussian distribution for the experimental and theoretical uncertainties. In Section 3 we estimate the goodness of fit using the Monte Carlo method, that is applicable in any case in which the distribution of the uncertainties is known (see, for example, Section 15.6 of Ref. [36]). In Section 4 we estimate with the Monte Carlo method the confidence level of the usual allowed regions in the $\tan^2\theta$–Δm^2 parameter space. In Section 5 we implement the classical frequentist Neyman method for finding exact confidence regions with correct coverage at a given confidence level.

3. Goodness of fit

In order to estimate the goodness of fit, our method proceeds as follows (see, for example, Section 15.6 of Ref. [36]). We estimate Δm^2, $\tan^2\theta$ through the minimum of X^2 in Eq. (1) and we call these observed best-fit values $\widehat{\Delta m^2}_{\rm obs}$, $\widehat{\tan^2\theta}_{\rm obs}$. Then we assume that $\widehat{\Delta m^2}_{\rm obs}$, $\widehat{\tan^2\theta}_{\rm obs}$ are reasonable surrogates of the true values $\Delta m^2_{\rm true}$, $\tan^2\theta_{\rm true}$ and the probability distribution of the differences $\widehat{\Delta m^2}_{(s)} - \widehat{\Delta m^2}_{\rm obs}$, $\widehat{\tan^2\theta}_{(s)} - \widehat{\tan^2\theta}_{\rm obs}$ is not too different from the true distribution of the differences $\widehat{\Delta m^2}_{(s)} - \Delta m^2_{\rm true}$, $\widehat{\tan^2\theta}_{(s)} - \tan^2\theta_{\rm true}$ in a large set of best-fit parameters $\widehat{\Delta m^2}_{(s)}$, $\widehat{\tan^2\theta}_{(s)}$ $(s = 1, 2, \ldots)$ obtained with hypothetical experiments.

Using $\widehat{\Delta m^2}_{\rm obs}$, $\widehat{\tan^2\theta}_{\rm obs}$ as surrogates of the true values, we generate N_s synthetic random data sets with the usual gaussian distribution for the experimental and theoretical uncertainties. We apply the least-squares method to each synthetic data set, leading to an ensemble of simulated best-fit parameters $\widehat{\Delta m^2}_{(s)}$, $\widehat{\tan^2\theta}_{(s)}$ with $s = 1, \ldots, N_s$, each one with his associated $(X^2_{\rm min})_s$. Then we calculate the goodness of fit as the fraction of simulated $(X^2_{\rm min})_s$ in the ensemble that are larger than the one actually observed, $(X^2_{\rm min})_{\rm obs}$.

We calculate the synthetic data sets generating random neutrino fluxes ϕ_i with a multinormal distribution centered on the SSM fluxes $\phi_i^{\rm SSM}$ and having the covariance matrix

$$V^{(\phi)}_{i_1,i_2} = \phi_i^{\rm SSM}\phi_{i_2}^{\rm SSM}\sum_k \alpha_{i_1k}\alpha_{i_2k}(\Delta \ln X_k)^2. \quad (9)$$

We also generate random energy-averaged cross-sections C_{ij} with a multinormal distribution centered on the theoretical energy-averaged cross-sections $C^{(\rm thr)}_{ij}$ corresponding to $\widehat{\Delta m^2}_{\rm obs}$, $\widehat{\tan^2\theta}_{\rm obs}$ and having the completely correlated covariance matrix for each independent experiment j

$$V^{(j)}_{i_1,i_2} = C^{(\rm thr)}_{i_1 j}\Delta \ln C^{(\rm thr)}_{i_1 j} C^{(\rm thr)}_{i_2 j}\Delta \ln C^{(\rm thr)}_{i_2 j}. \quad (10)$$

Then, we calculate the rates $R_j = \sum_i \phi_i C_{ij}$. Finally, we generate random synthetic experimental rates $R_j^{(s)}$ with normal distribution centered on R_j and standard deviation equal to that of the actual experimental data (σ_j). The synthetic experimental rates are inserted in the least-squares function (1) in place of $R_j^{(\rm exp)}$ in order to find the minimum $(X^2_{\rm min})_s$ and its associated best-fit parameters $\widehat{\Delta m^2}_{(s)}$, $\widehat{\tan^2\theta}_{(s)}$.

The global minimum of the least-squares function (1), $(X^2_{\rm min})_{\rm obs} = 0.42$, occurs in the SMA region for $\widehat{\Delta m^2}_{\rm obs} = 5.1\times10^{-6}$ eV^2 and $\widehat{\tan^2\theta}_{\rm obs} = 1.6\times10^{-3}$, from which we obtained the estimations of the goodness of fit listed in Table 1. We first restricted the values of the mixing parameters in the area

$$10^{-4} \leqslant \tan^2\theta \leqslant 3\times10^{-2},$$
$$3\times10^{-7} \leqslant \Delta m^2 \leqslant 10^{-4}\text{eV}^2 \quad (\overline{\text{SMA}}\text{ area}), \quad (11)$$

around the SMA region, obtaining the Monte Carlo estimate of the goodness of fit reported in the $\overline{\text{SMA}}$ column of Table 1. This value is almost

Table 1
Monte Carlo estimate of the goodness of fit of solar neutrino data calculated with 10^6 synthetic data sets

	Standard GOF	Monte Carlo GOF		
		$\overline{\text{SMA}}$	$\overline{\text{MSW}}$	$\overline{\text{MSW}}+\overline{\text{VO}}$
$(X^2_{\rm min})_{\rm obs} = 0.42$ $\widehat{\Delta m^2}_{\rm obs} = 5.1\times10^{-6}$ eV^2 $\widehat{\tan^2\theta}_{\rm obs} = 1.6\times10^{-3}$	51.8%	53.7%	48.4%	39.6%

In the $\overline{\text{SMA}}$, $\overline{\text{MSW}}$, $\overline{\text{MSW}}+\overline{\text{VO}}$ columns the values of the neutrino oscillation parameters are restricted, respectively, in the $\overline{\text{SMA}}$, $\overline{\text{MSW}}$, $\overline{\text{MSW}}+\overline{\text{VO}}$ areas (see Eqs. (6), (7) and (11)).

equal (even slightly larger) to the standard one obtained assuming a χ^2 distribution with one degree of freedom, reported in the "Standard GOF" column of Table 1. Hence, we conclude that locally the usual method to evaluate the goodness of fit is reliable.

However, when we extend the allowed region of the mixing parameters to all the $\overline{\text{MSW}}$ area (6) and when we add also the $\overline{\text{VO}}$ area (7), we obtain the values reported, respectively, in the $\overline{\text{MSW}}$ and $\overline{\text{MSW}} + \overline{\text{VO}}$ columns of Table 1, which are significantly smaller than the one obtained with the standard method. As remarked in Section 2, this is mainly due to the non-linear dependence of the theoretical rates from the neutrino oscillation parameters, that implies that there are more possibilities to obtain good fits of the data with respect to the linear case. Therefore, we conclude that the standard method, although valid locally (when the allowed region of the parameters is restricted around the SMA region the linear assumption is approximately correct), is not valid in general and should not be trusted if there is more than one allowed region.

In order to check the local validity of the standard method we have also assumed that $\widehat{\Delta m^2}_{\text{obs}}$ and $\widehat{\tan^2\theta}_{\text{obs}}$ have the values corresponding to the local minima of X^2 in the LMA, LOW and VO regions, restricting the values of the parameters around the corresponding areas:

$$3\times10^{-2}\leqslant\tan^2\theta\leqslant2,\quad 2\times10^{-6}\leqslant\Delta m^2\leqslant10^{-3}\text{eV}^2 \quad (\overline{\text{LMA}}\text{ area}), \tag{12}$$

$$3\times10^{-2}\leqslant\tan^2\theta\leqslant2,\quad 10^{-8}\leqslant\Delta m^2\leqslant2\times10^{-6}\text{eV}^2, \quad (\overline{\text{LOW}}\text{ area}), \tag{13}$$

and the $\overline{\text{VO}}$ area in Eq. (7). The results are reported in Table 2. One can see that the standard method is locally acceptable for the LMA and LOW solutions, but it largely over-estimates the goodness of fit in the case of the VO solution. This is due to the fact that the theoretical rates are highly non-linear functions of the neutrino oscillation parameters in the VO region (7), resulting in several disconnected allowed regions.

Summarizing the results of this section, we have shown that if there were only one allowed region in the space of the neutrino oscillation parameters, or if there are valid reasons to restrict the allowed region of the parameters around one of the SMA, LMA, LOW solutions, the standard method to calculate the goodness of fit is approximately reliable. On the other hand, if there are more than one allowed regions, the standard method to calculate the goodness of fit is not reliable and the goodness of fit should be estimated numerically, with Monte Carlo, as we have done. This happens if one considers the $\overline{\text{MSW}}$ region (6) of the neutrino oscillation parameters, which contains three allowed regions (SMA, LMA and LOW), or the $\overline{\text{VO}}$ region (7), that contains several allowed regions, or all the parameter space ($\overline{\text{MSW}} + \overline{\text{VO}}$).

Table 2
Monte Carlo estimate of the local goodness of fit of solar neutrino data in the $\overline{\text{LMA}}$, $\overline{\text{LOW}}$ and $\overline{\text{VO}}$ areas (see Eqs. (7), (12) and (13)) calculated with 10^6 synthetic data sets

	Area	Standard GOF	Monte Carlo GOF
$\overline{\text{LMA}}$	$(X^2_{\text{min}})_{\text{obs}} = 3.46$ $\widehat{\Delta m^2}_{\text{obs}} = 1.5\times10^{-5}\ \text{eV}^2$ $\widehat{\tan^2\theta}_{\text{obs}} = 0.30$	6.3%	6.1%
$\overline{\text{LOW}}$	$(X^2_{\text{min}})_{\text{obs}} = 6.53$ $\widehat{\Delta m^2}_{\text{obs}} = 1.3\times10^{-7}\ \text{eV}^2$ $\widehat{\tan^2\theta}_{\text{obs}} = 0.55$	1.1%	1.9%
$\overline{\text{VO}}$	$(X^2_{\text{min}})_{\text{obs}} = 1.29$ $\widehat{\Delta m^2}_{\text{obs}} = 9.4\times10^{-11}\ \text{eV}^2$ $\widehat{\tan^2\theta}_{\text{obs}} = 0.38$	25.6%	14.2%

4. Confidence level of allowed regions

In order to calculate the confidence level of the allowed regions it is necessary first to understand what is its meaning. The 100β% CL allowed regions are defined by the property that they belong to a set of allowed regions obtained with hypothetical experiments and the regions belonging to this set cover (i.e. include) the true value of the parameters with probability β.

Given the usual "100β% CL" allowed regions in the space of the neutrino oscillation parameters we

can calculate their Monte Carlo confidence level β_{MC} with a method similar to the one described in the previous section for the goodness of fit. We assume that $\widehat{\Delta m^2}_{obs}$, $\widehat{\tan^2\theta}_{obs}$ are reasonable surrogates of the true values Δm^2_{true}, $\tan^2\theta_{true}$ and we generate a large number of synthetic data sets. We apply the standard procedure to each synthetic data set and obtain the corresponding $100\beta\%$ CL allowed regions in the space of the neutrino oscillation parameters. Then we count the number of synthetic $100\beta\%$ CL allowed regions that cover the assumed surrogate $\widehat{\Delta m^2}_{obs}$, $\widehat{\tan^2\theta}_{obs}$ of the true values. The ratio of this number and the total number of synthetically generated data set gives the confidence level β_{MC} of the $100\beta\%$ CL allowed regions.

The results of our Monte Carlo estimation of the confidence level of the standard allowed regions shown in Figs. 1 and 2 are reported in Table 3. The values of $\widehat{\Delta m^2}_{obs}$, $\widehat{\tan^2\theta}_{obs}$ used as surrogates of the true values of the parameters are those of the global minimum of the least-squares function (1), given in Table 1. As we have done in the previous section for the goodness of fit, we calculated first the confidence level of the SMA region restricting the values of the parameters in the $\overline{\text{SMA}}$ area (11) ($\overline{\text{SMA}}$ column of Table 3). Then we calculated the confidence level of the SMA + LMA + LOW regions (shown in Fig. 1) restricting the values of the parameters to the $\overline{\text{MSW}}$ area (6) ($\overline{\text{MSW}}$ column of Table 3). Finally, we calculated the confidence levels of all the allowed regions in the $\overline{\text{MSW}} + \overline{\text{VO}}$ area shown in Figs. 1 and 2 ($\overline{\text{MSW}} + \overline{\text{VO}}$ column of Table 3).

From Table 3 one can see that the value of the confidence level of the standard SMA region calculated locally, in the $\overline{\text{SMA}}$ area (11), practically coincides with the nominal value ("Standard CL" column of Table 3). However, when the allowed values of the parameters are extended to the whole $\overline{\text{MSW}}$ area (6) or to the $\overline{\text{MSW}} + \overline{\text{VO}}$ area, the confidence level of the allowed regions (SMA+ LMA + LOW in the $\overline{\text{MSW}}$ area and SMA+ LMA + LOW + VO in the $\overline{\text{MSW}} + \overline{\text{VO}}$ area) is significantly smaller than its nominal value. For example, the Monte Carlo confidence level of the standard 90% CL SMA + LMA + LOW + VO region in the $\overline{\text{MSW}} + \overline{\text{VO}}$ area is 86.44%.

Let us consider now the possible existence of a reason to restrict the values of the oscillation parameters in the $\overline{\text{LMA}}$, $\overline{\text{LOW}}$, or $\overline{\text{VO}}$ area (defined, respectively, in Eqs. (7), (12) and (13)). In this case, if the local goodness of fit is considered to be acceptable, one can calculate the corresponding standard local allowed regions of the parameters with the prescription (5) in which $(X^2_{min})_{obs}$ is the observed local minimum of the least-squares function (1). Considering the actual value of the local goodness of fit in the $\overline{\text{LMA}}$, $\overline{\text{LOW}}$, and $\overline{\text{VO}}$ areas given in Table 2 to be acceptable, the corresponding standard local LMA, LOW and VO allowed regions are those presented, respectively, in Figs. 3–5. Obviously, they are larger than the corresponding ones in Figs. 1 and 2 and they exist for any value of the confidence level, whereas, for example, in Fig. 1 there is no LOW region at 90% CL.

The Monte Carlo estimation of the confidence level of the standard local LMA, LOW and VO allowed regions is presented in Table 4. One can see that the Monte Carlo confidence levels of the

Table 3
Monte Carlo estimate of the confidence level of the standard 90%, 95%, 99% and 99.73% CL allowed regions shown in Figs. 1 and 2[a]

Standard CL	Monte Carlo CL		
	$\overline{\text{SMA}}$	$\overline{\text{MSW}}$	$\overline{\text{MSW}} + \overline{\text{VO}}$
90.00% (1.64σ)	90.11% (1.65σ)	87.22% (1.52σ)	86.44% (1.49σ)
95.00% (1.96σ)	95.01% (1.96σ)	93.08% (1.82σ)	92.75% (1.80σ)
99.00% (2.58σ)	99.00% (2.58σ)	98.51% (2.43σ)	98.42% (2.41σ)
99.73% (3.00σ)	99.72% (2.99σ)	99.58% (2.86σ)	99.56% (2.85σ)

[a] The Monte Carlo confidence levels have been calculated generating 10^6 synthetic data sets. The $\overline{\text{SMA}}$, $\overline{\text{MSW}}$, $\overline{\text{MSW}} + \overline{\text{VO}}$ columns report the Monte Carlo estimations of the confidence levels calculated by restricting the values of the parameters in the $\overline{\text{SMA}}$, $\overline{\text{MSW}}$, $\overline{\text{MSW}} + \overline{\text{VO}}$ areas (see Eqs. (6), (7) and (11)).

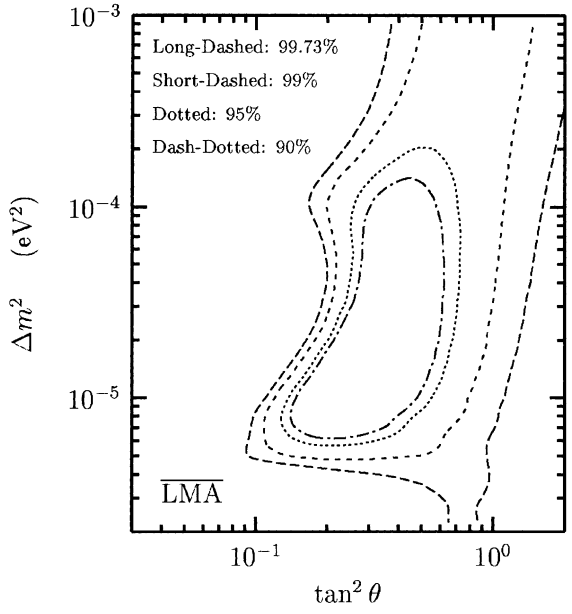

Fig. 3. Local standard 90% (1.6σ), 95% (2σ), 99% (2.6σ) and 99.73% (3σ), CL allowed regions in the $\overline{\text{LMA}}$ area (12).

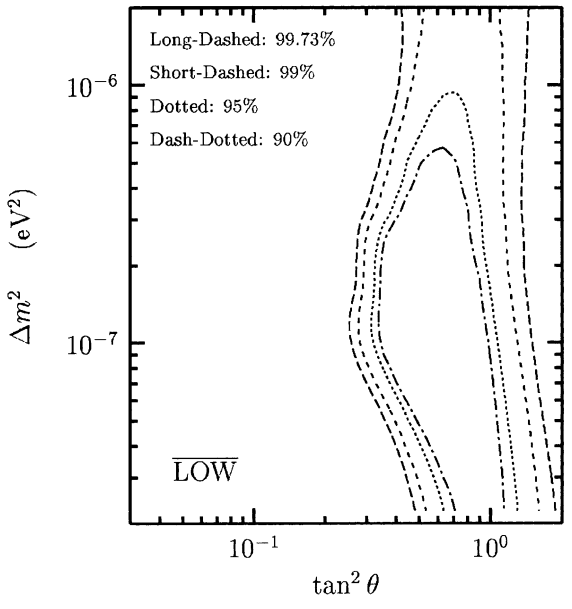

Fig. 4. Local standard 90% (1.6σ), 95% (2σ), 99% (2.6σ) and 99.73% (3σ), CL allowed regions in the $\overline{\text{LOW}}$ area (13).

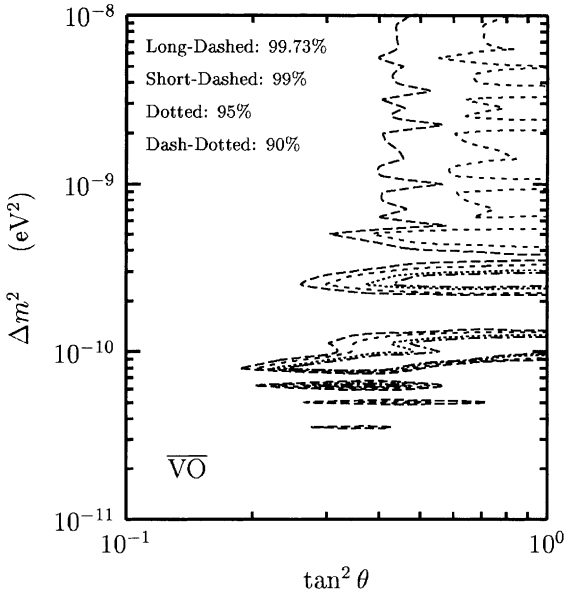

Fig. 5. Local standard 90% (1.6σ), 95% (2σ), 99% (2.6σ) and 99.73% (3σ), CL allowed regions in the $\overline{\text{VO}}$ area (7).

Table 4
Monte Carlo estimate of the confidence level of the local 90%, 95%, 99% and 99.73% CL allowed regions shown in Figs. 3–5 in which the values of the parameters are restricted in the $\overline{\text{LMA}}$, $\overline{\text{LOW}}$ or $\overline{\text{VO}}$ areas (see Eqs. (7), (12) and (13))[a]

Area	Standard CL	Monte Carlo CL
$\overline{\text{LMA}}$	90.00% (1.64σ)	89.86% (1.64σ)
	95.00% (1.96σ)	94.93% (1.95σ)
	99.00% (2.58σ)	98.99% (2.57σ)
	99.73% (3.00σ)	99.73% (3.00σ)
$\overline{\text{LOW}}$	90.00% (1.64σ)	92.53% (1.78σ)
	95.00% (1.96σ)	96.39% (2.10σ)
	99.00% (2.58σ)	99.33% (2.71σ)
	99.73% (3.00σ)	99.82% (3.12σ)
$\overline{\text{VO}}$	90.00% (1.64σ)	86.29% (1.49σ)
	95.00% (1.96σ)	92.99% (1.81σ)
	99.00% (2.58σ)	98.68% (2.48σ)
	99.73% (3.00σ)	99.69% (2.96σ)

[a] The Monte Carlo confidence levels have been calculated generating 10^6 synthetic data sets.

standard local LMA and LOW regions are similar to their nominal values (with small deviations with unpredictable sign). On the other hand, the Monte Carlo confidence level of the standard local VO region is significantly smaller than its nominal

value. This is due to the fact that the linear approximation assumed for the calculation of the standard confidence levels is badly violated (there are several disconnected allowed VO regions).

Summarizing the results of this section, we have shown that the standard confidence levels of the allowed regions in the neutrino oscillation parameter space are approximately correct if only one of the SMA, LMA or LOW region is considered to be allowed a priori. If the oscillation parameters are restricted to the $\overline{\text{MSW}}$ area (6), the confidence levels are significantly smaller than the standard ones. If one does not impose any restriction on the values of the parameters, the confidence levels decrease further. If only the $\overline{\text{VO}}$ area is considered to be allowed, the confidence level of the local standard allowed regions is significantly smaller than the standard one, because of the multiplicity of allowed regions.

5. Exact allowed regions

In the previous section we estimated the confidence level of the allowed regions in the neutrino oscillation parameter space obtained with the standard procedure based on Eq. (5). This estimation is approximate, because it is based on the assumption of a surrogate for the unknown true values of the neutrino oscillation parameters.

Luckily, there is a well-known procedure for constructing exact allowed regions independently of the true values of the parameters. This procedure has been invented by Neyman in 1937 [39] (see also Refs. [34,40,41]). It guarantees that the resulting allowed regions have correct frequentist *coverage* (see Refs. [42–46]), i.e. they belong to a set of allowed regions obtained with different or similar, real or hypothetical experiments that cover the true values of the parameters with the desired probability given by the chosen confidence level. In this section we apply this method in order to find allowed regions with proper coverage for the neutrino oscillation parameters.

Neyman's construction of exact frequentist allowed regions with $100\beta\%$ confidence level starts with the choice of appropriate estimators of the parameters under investigation. Then, for any possible value of the parameters one calculates the corresponding *acceptance zone*[5] with probability β, i.e. regions in the space of the estimators that contain $100\beta\%$ of the values of the estimators obtained in a large series of trails. Several methods are available for the construction of the acceptance zones (see Refs. [34,40,41,43,45,46] and references therein). If the probability distributions of the estimators are known, the acceptance zones can be calculated analytically; if not, one can calculate probability distributions of the estimators and the acceptance zones with numerical Monte Carlo methods.

Once the $100\beta\%$ acceptance zone for each possible value of the parameters are calculated, the $100\beta\%$ allowed regions are simply composed by all the parameters values whose acceptance zone covers the measured value of the estimators (i.e. the actual estimate of the parameters). If the acceptance zones are composed by disconnected subzones, also the allowed region may be composed by disconnected allowed sub-regions. As we will see in the following, this is what happens in the case of solar neutrino oscillations.

Our implementation of Neyman's construction goes as follows:

1. We choose the standard estimator of the neutrino oscillation parameters: the value $\widehat{\tan^2\theta}$, $\widehat{\Delta m^2}$ of the parameters in the minimum of the least-squares function (1).

2. Since the probability distribution of $\widehat{\tan^2\theta}$, $\widehat{\Delta m^2}$ for each possible value of the parameters $\tan^2\theta$, Δm^2 is not known, we calculate it numerically with a Monte Carlo.

   (a) We define an appropriate grid in the 2-dimensional space of the neutrino oscillation parameters $\tan^2\theta$, Δm^2.
   (b) For each Δm^2, $\tan^2\theta$ on the grid we generate a large number of synthetic data sets labeled by

[5] The acceptance zones and the allowed regions become, respectively, acceptance intervals and confidence intervals in the simplest case of one parameter, which is discussed in most textbooks (see Refs. [34,40]).

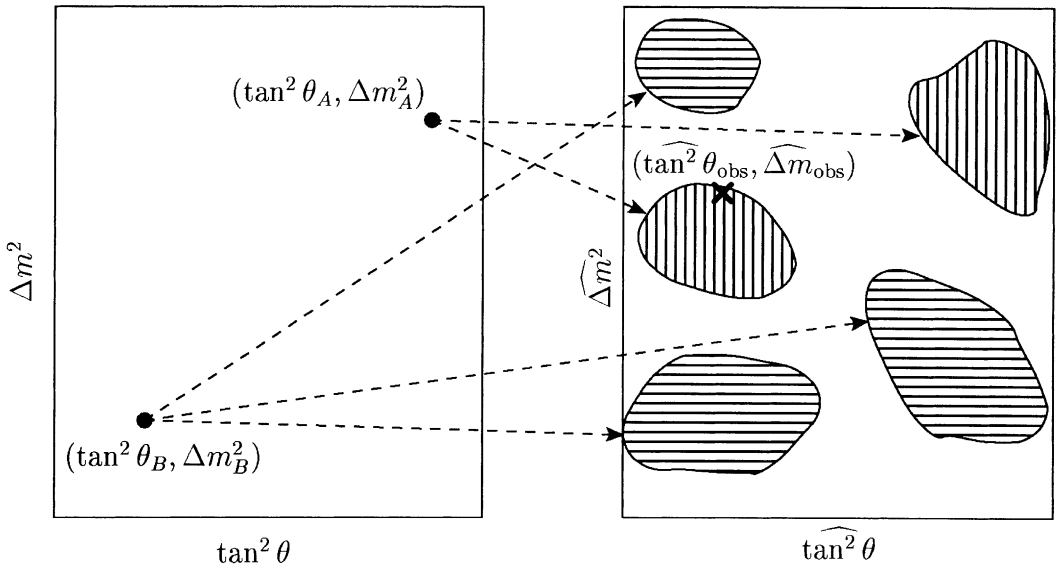

Fig. 6. Illustration of the acceptance zones in the $\widehat{\tan^2\theta}$–$\widehat{\Delta m^2}$ generated by the two pairs $(\tan^2\theta_A, \Delta m^2_A)$ and $(\tan^2\theta_B, \Delta m^2_B)$ of parameters. The cross corresponds to the observed values $(\widehat{\tan^2\theta}_{\rm obs}, \widehat{\Delta m^2}_{\rm obs})$. The two vertically hatched regions constitute the acceptance zone associated with $(\tan^2\theta_A, \Delta m^2_A)$. Since the observed value $(\widehat{\tan^2\theta}_{\rm obs}, \widehat{\Delta m^2}_{\rm obs})$ lies in one of the vertically hatched regions, $(\tan^2\theta_A, \Delta m^2_A)$ is included in the allowed region. The three horizontally hatched regions constitute the acceptance zone associated with $\tan^2\theta_B, \Delta m^2_B$. Since the observed value $(\widehat{\tan^2\theta}_{\rm obs}, \widehat{\Delta m^2}_{\rm obs})$ lies outside all the horizontally hatched regions, $(\tan^2\theta_B, \Delta m^2_B)$ is excluded from the allowed region.

the index $s = 1, \ldots, N_s$. These synthetic data sets are generated randomly using the method described in Section 3.

(c) For each synthetic data set we find the values $\widehat{\tan^2\theta}_{(s)}$ and $\widehat{\Delta m^2}_{(s)}$ corresponding to the minimum of the least-squares function (1).This procedure gives the distribution of $\widehat{\tan^2\theta}$ and $\widehat{\Delta m^2}$ for each point on the grid in the space of the neutrino oscillation parameters. Unfortunately this is a rather lengthy task that requires several days of computer time in order to reach an acceptable accuracy, essentially because of the large number of points on a reasonably fine grid, about five thousand in the $\overline{\rm MSW}$ region (6) and six thousand in the $\overline{\rm VO}$ region (7).

3. In our procedure, the acceptance zones are 2-dimensional regions in the $\widehat{\tan^2\theta}$–$\widehat{\Delta m^2}$ space, as illustrated qualitatively in Fig. 6.

For each point on the grid we calculate the corresponding $100\beta\%$ acceptance zone in the simplest and most natural way:[6] we choose the smallest possible acceptance zone, i.e. that containing the values of $\widehat{\tan^2\theta}$–$\widehat{\Delta m^2}$ with highest probability, whose sum is equal to β. In the case of a linear least-squares fit this method gives the allowed regions obtained with the standard prescription (5). Therefore, our exact allowed regions can be compared directly with the standard ones. Furthermore, in the case of a symmetric distribution, the method of smallest acceptance zones corresponds to the one-dimensional method of central intervals which is known to be uniformly most powerful unbiased for distributions belong-

[6] There is a subtle problem in choosing the method that defines the acceptance zones: the method must be chosen independently of the data and the result. This is what we have done. Otherwise, the property of coverage is lost (see Refs. [41–46]), and one can always choose a method "ad hoc" to obtain any desired result.

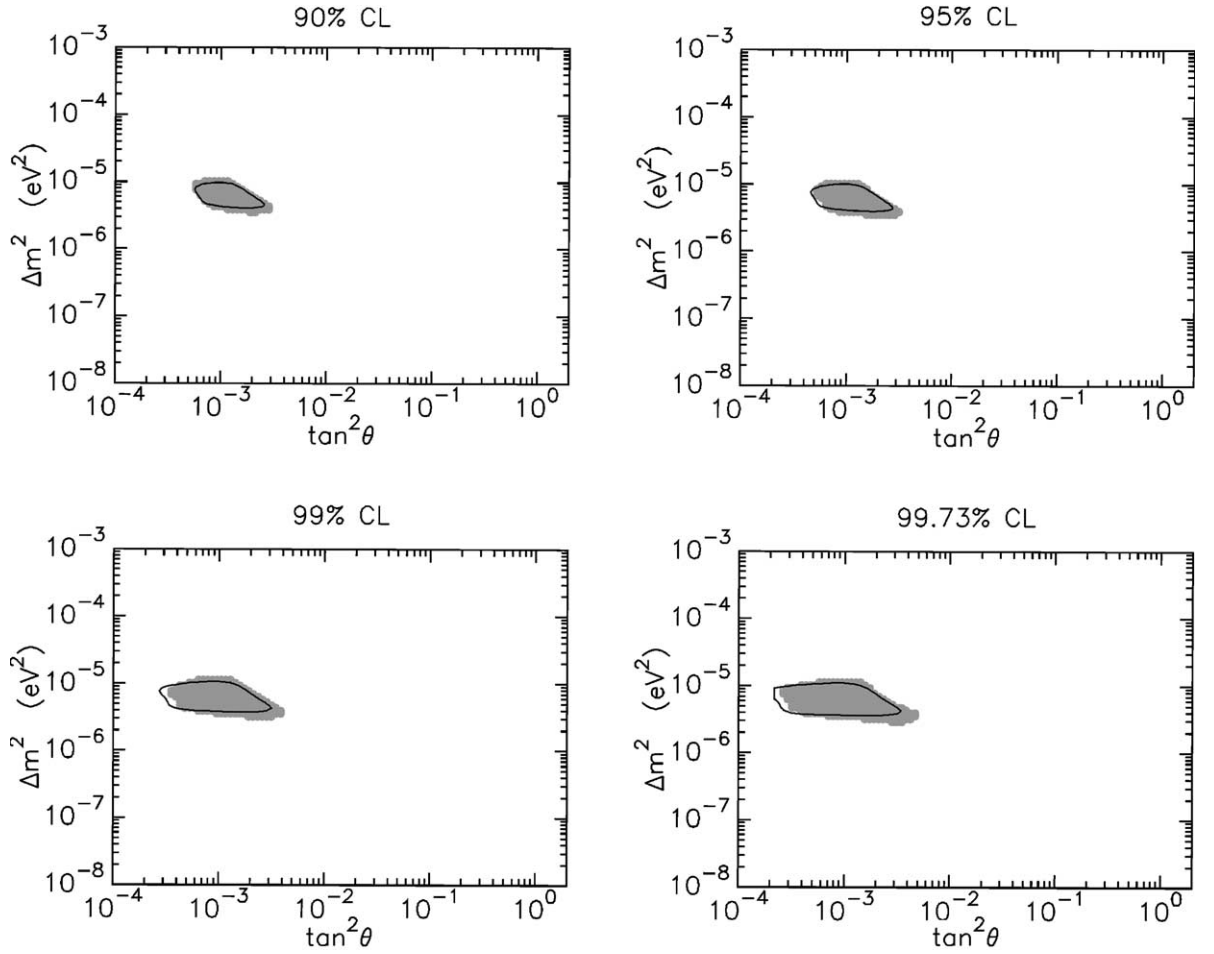

Fig. 7. Allowed 90%, 95%, 99%, 99.73% confidence level regions in the $\tan^2\theta$–Δm^2 plane. In each plot the gray area is the allowed region with exact frequentist coverage obtained restricting the possible values of $\tan^2\theta$ and Δm^2 in the $\overline{\text{SMA}}$ area (11) around the SMA solution, where $(X^2_{\text{min}})_{\text{obs}}$ lies. The area enclosed by the solid line is the standard SMA allowed region, shown also in Fig. 1.

ings to the exponential family (see Ref. [40]). A study of the properties of this method will be presented elsewhere [7].

4. We calculate the allowed regions in the $\tan^2\theta$–Δm^2 plane by taking all the values of the parameters whose acceptance zone includes $(\widehat{\tan^2\theta}_{\text{obs}}, \widehat{\Delta m^2}_{\text{obs}})$ (the measured value of the estimator, called "estimate").

Because of the non-linearity of the neutrino oscillation probability as a function of the parameters, the acceptance zones are composed by disconnected sub-zones. This generates two-dimensional allowed regions composed by disconnected allowed sub-regions, some of which lie far from $(\widehat{\tan^2\theta}_{\text{obs}}, \widehat{\Delta m^2}_{\text{obs}})$.

The last step of the procedure is illustrated qualitatively in Fig. 6, where the cross corresponds to the observed $(\widehat{\tan^2\theta}_{\text{obs}}, \widehat{\Delta m^2}_{\text{obs}})$, the union of the two vertically hatched regions is the acceptance zone associated with $(\tan^2\theta_A, \Delta m^2_A)$, and the union of the three horizontally hatched regions is the acceptance zone associated with $(\tan^2\theta_B, \Delta m^2_B)$. Since the acceptance zone associated with $(\tan^2\theta_A, \Delta m^2_A)$ includes $(\widehat{\tan^2\theta}_{\text{obs}}, \widehat{\Delta m^2}_{\text{obs}})$, the point $(\tan^2\theta_A, \Delta m^2_A)$ is included in the allowed region. On the other hand, since the acceptance zone associated

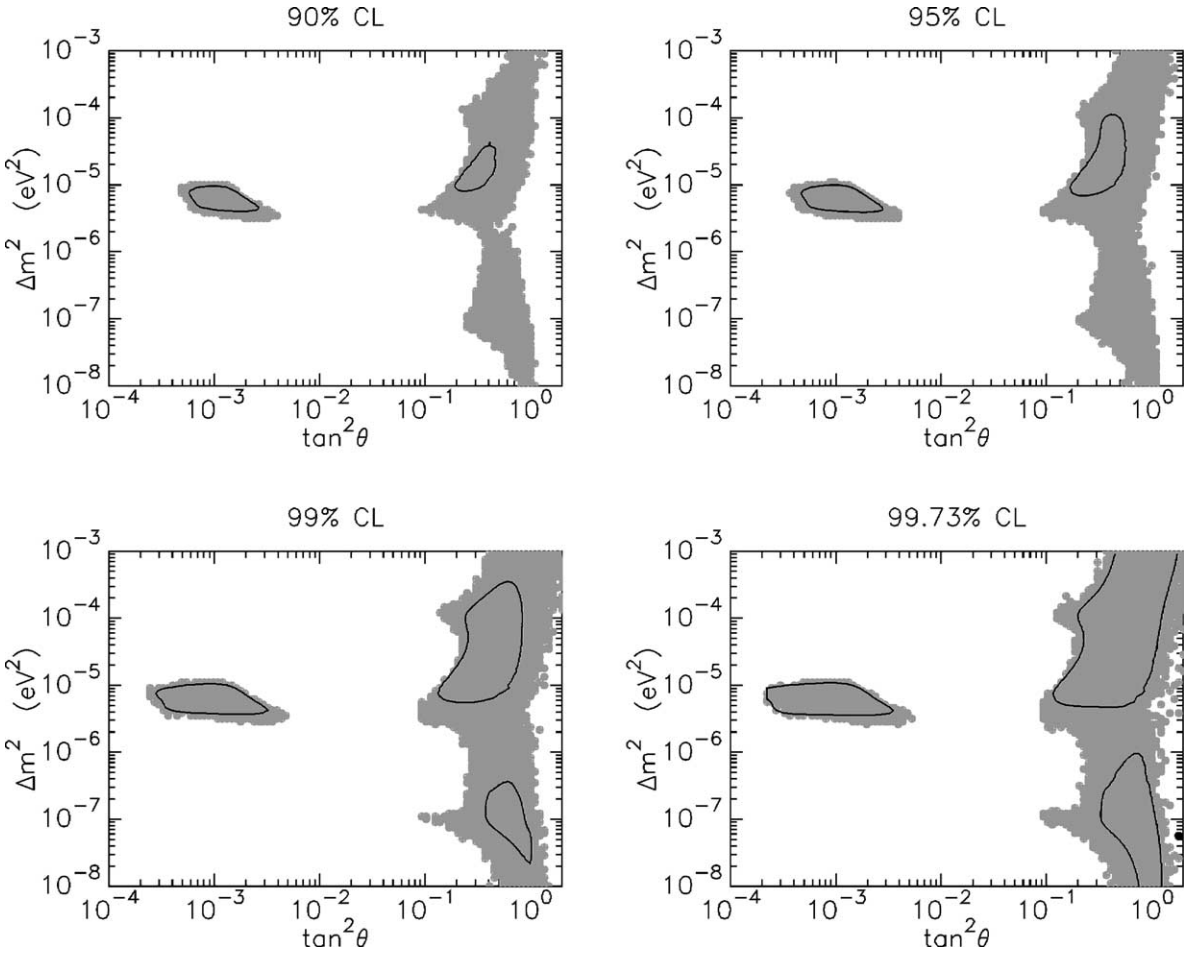

Fig. 8.

with $(\tan^2\theta_B, \Delta m^2_B)$ does not include $(\widehat{\tan^2\theta}_{\rm obs}, \widehat{\Delta m^2}_{\rm obs})$, the point $(\tan^2\theta_B, \Delta m^2_B)$ is excluded from the allowed region.

The results of our calculations are presented in Figs. 7–10, where we have depicted the 90%, 95%, 99% and 99.73% CL regions (gray areas) confronted with those obtained with the standard method based on Eq. (5) (areas enclosed by solid lines), where $(X^2_{\rm min})_{\rm obs}$ is the global minimum of the least-squares function (1), which lies in the SMA region. The standard regions coincide with those shown in Figs. 1 and 2.

In Fig. 7 we have restricted the possible values of the neutrino oscillation parameters in the SMA area (11) around the SMA solution, where $(X^2_{\rm min})_{\rm obs}$ lies. The acceptance zone for each point on the grid in the parameter space has been calculated generating about 6×10^5 synthetic data sets (different for different points on the grid, in order to avoid correlations). One can see that the standard allowed SMA region is an acceptable approximation of the exact [7] allowed region. This is due to the fact that locally the linear approxi-

[7] Here the adjective "exact" refers to the method, that produces allowed regions with exact coverage. Obviously our allowed regions are approximations of the exact ones, that would be obtained with an infinitely dense grid in parameter space and an infinite set of synthetic random data sets.

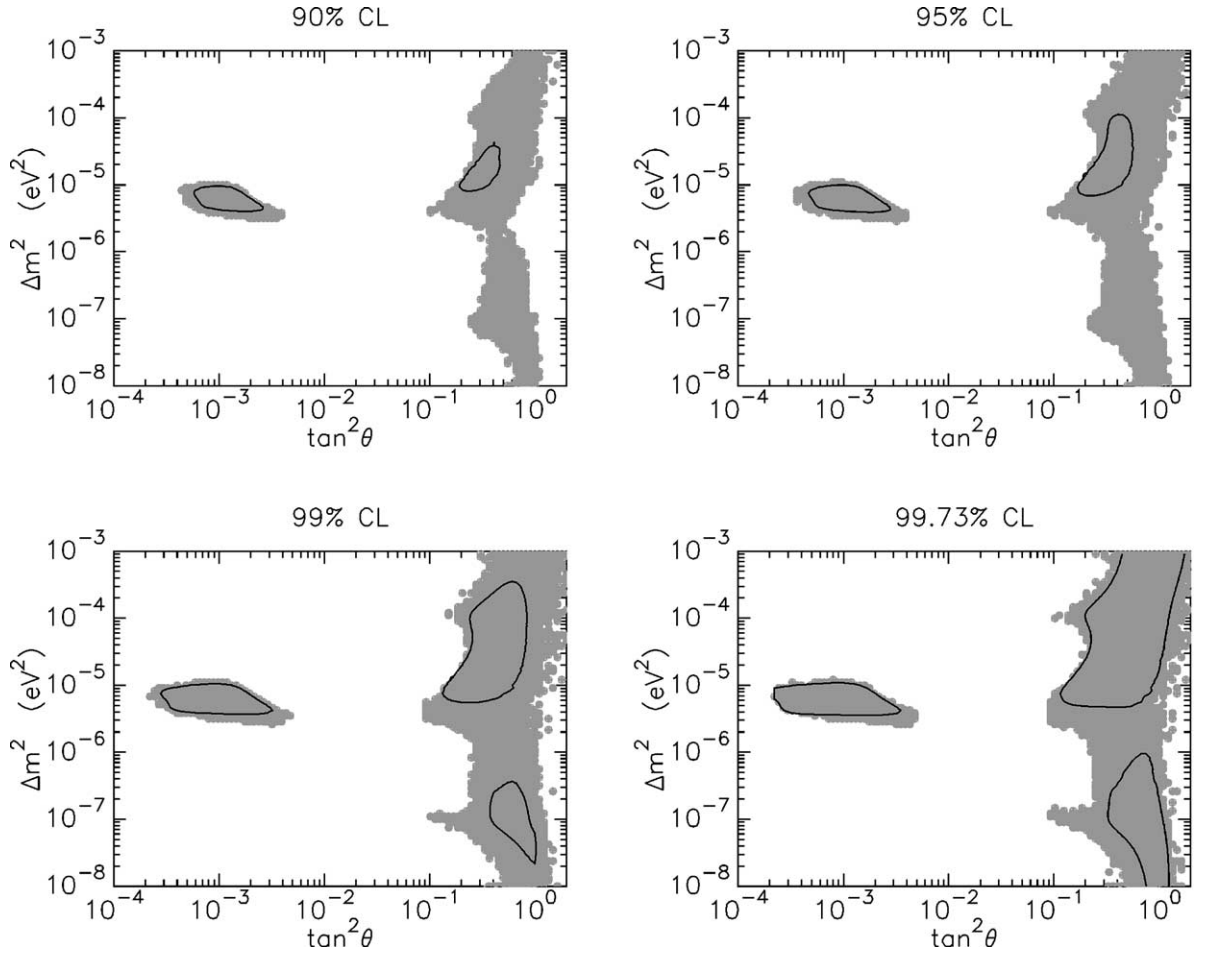

Fig. 9.

mation is rather good, as we already found in the previous two sections.

In Fig. 8 we have extended the possible values of the neutrino oscillation parameters to all the $\overline{\text{MSW}}$ area (6). For this figure the number of synthetic data sets for each point on the grid is about 7×10^4 (less than in Fig. 7 because of the larger size of the grid, that slows down the calculation). The standard SMA region is still an acceptable approximation of the exact SMA region, but the exact LMA and LOW regions are larger than the standard ones, so large that they merge together, producing a large allowed region around maximal mixing ($\tan^2\theta = 1$). This behavior can be understood by comparing Fig. 8 with Fig. 1, which shows that the standard LMA and LOW regions merge at high confidence level (99.95% CL, corresponding to 3.5σ). As we have shown in Section 4, the confidence level of the standard allowed region is smaller than its nominal value. Therefore, it is natural to expect that the exact allowed regions bear some resemblance with the standard regions calculated at higher confidence level.

Figs. 9 and 10 show, respectively, the allowed MSW and VO regions when there is no restriction on the possible values of the neutrino oscillations parameters (the number of synthetic data sets for

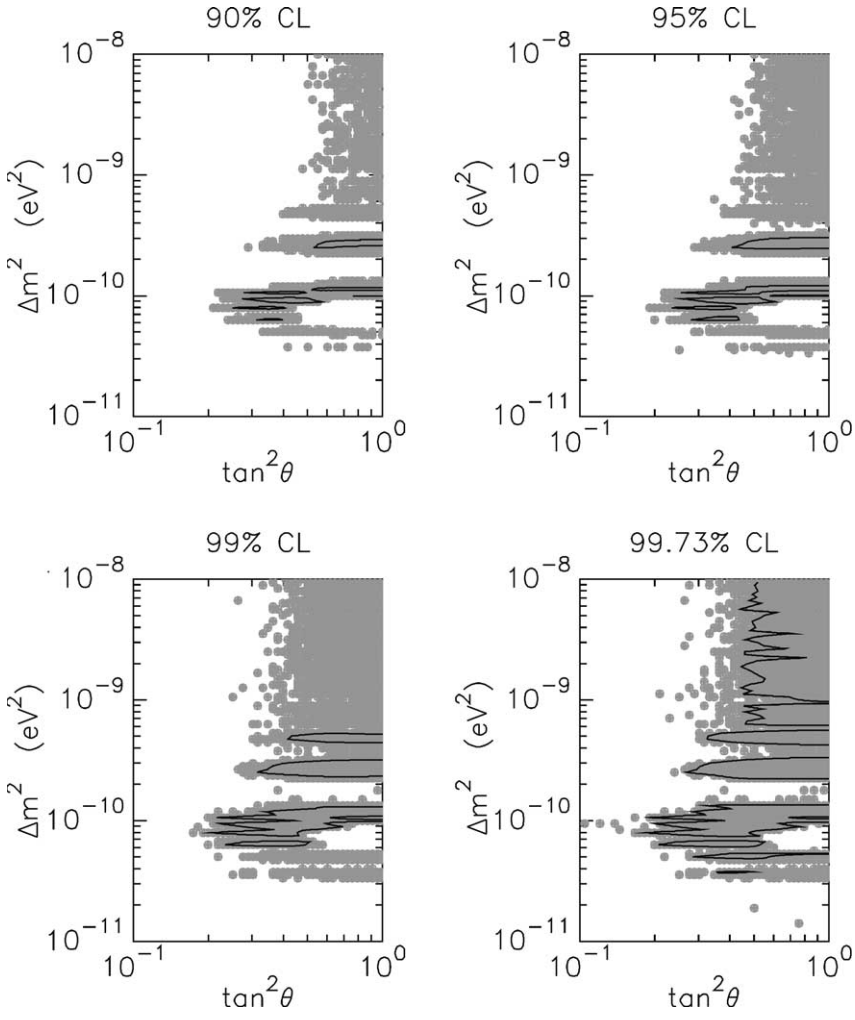

Fig. 10.

each point on the grid is now about 6.5×10^4). [8] Again, one can see that the standard SMA region is an acceptable approximation of the exact SMA region, but the exact LMA, LOW and VO regions are much larger than the standard ones.

From the results of our calculations we conclude that the standard method to calculate allowed regions produces reliable results only locally, i.e. in the calculation of the allowed region surrounding the global minimum of X^2. The other allowed regions are underestimated by the standard method.

6. Conclusions

We have presented the results of a numerical Monte Carlo calculation of the goodness of fit and the confidence level of the standard allowed regions for the neutrino oscillation parameters Δm^2,

[8] For all Figs. 7–10 we have verified that the number of synthetic data sets is sufficient to reach convergence, by comparing the results obtained with different numbers of synthetic data sets.

$\tan^2\theta$ obtained from the fit of solar neutrino data. We have shown that the standard values of the goodness of fit and of the confidence level of the allowed regions are significantly overestimated with the standard method. This is mainly due to the non-linear dependence of the neutrino oscillation probability from the parameters. The linear approximation, leading to the standard values of the goodness of fit and of the confidence level of the allowed regions, is valid only locally, for values of the parameters around a specific MSW solution (SMA, LMA, LOW). In the case of the VO solutions the linear approximation is not valid even locally, because of the strong non-linearity of the oscillation probability that causes the existence of several allowed regions close together.

We have also calculated exact allowed regions with correct frequentist coverage using Neyman's method. The result of these calculations show that the standard allowed region around the global minimum of the least-squares function is a reasonable approximation of the exact one. On the other hand, the size of the other regions is underestimated in the standard method. Indeed, in our calculation the exact SMA region, that contains the minimum of the least-squares function, practically coincides with the standard one. On the other hand, the exact LMA and LOW regions are much larger than the standard ones, so much that they merge in a large allowed region around maximal mixing. Also the exact allowed VO regions are much larger than the standard ones.

The indications on neutrino mixing coming from solar neutrino data are becoming increasingly important for theory and experiment. Furthermore, solar neutrino data will soon be enriched by results of new powerful experiments (SNO [47], BOREXINO [48], GNO [49] and others [50]). As we have shown, the standard statistical analysis of solar neutrino data can lead to imprecise conclusions concerning the goodness of fit, the confidence level of the allowed regions and the size of the allowed regions far from the global minimum of the least-square function. Hence, we believe that it is time to examine critically the method of statistical analysis of solar neutrino data and bring it to the level of quality already attained in other branches of research in high-energy physics.

References

[1] B.T. Cleveland et al., Astrophys. J. 496 (1998) 505.
[2] Super-Kamiokande Collaboration, Y. Suzuki, XIX International Symposium on Lepton and Photon Interactions at High Energies, Stanford, 1999. http://www.sk.icrr.u-tokyo.ac.jp/doc/sk/pub/index.html.
[3] GALLEX, W. Hampel et al., Phys. Lett. B 447 (1999) 127.
[4] SAGE, J.N. Abdurashitov et al., Phys. Rev. C 60 (1999) 055801. Available from <astro-ph/9907113>.
[5] M.C. Gonzalez-Garcia, P.C. de Holanda, C. Pena-Garay, J.W.F. Valle, Nucl. Phys. B 573 (2000) 3. Available from <hep-ph/9906469>.
[6] Neutrino 2000, Sudbury, Canada, June 2000. http://nu2000.sno.laurentian.ca.
[7] M.V. Garzelli, C. Giunti, work in progress.
[8] S.M. Bilenky, S.T. Petcov, Rev. Mod. Phys. 59 (1987) 671.
[9] S.M. Bilenky, C. Giunti, W. Grimus, Prog. Part. Nucl. Phys. 43 (1999) 1. Available from <hep-ph/9812360>.
[10] A. de Gouvea, A. Friedland, H. Murayama, Phys. Lett. B 490 (2000) 125. Available from <hep-ph/0002064>.
[11] M.C. Gonzalez-Garcia, C Pena-Garay, Phys. Rev. D 62 (2000) 031301. Available from <hep-ph/0002186>.
[12] G.L. Fogli, E. Lisi, G. Scioscia, Phys. Rev. D 52 (1995) 5334. Available from <hep-ph/9506350>.
[13] G.L. Fogli, E. Lisi, D. Montanino, Phys. Rev. D 54 (1996) 2048. Available from <hep-ph/9605273>.
[14] G.L. Fogli, E. Lisi, D. Montanino, G. Sciosia, Phys. Rev. D 56 (1997) 4365. Available from <hep-ph/9706230>.
[15] C. Giunti, M.C. Gonzalez-Garcia, C. Pena-Garay, Phys. Rev. D 62 (2000) 013005. Available from <hep-ph/0001101>.
[16] S.P. Mikheyev, A.Yu. Smirnov, Yad. Fiz. 42 (1985) 1441 (Sov. J. Nucl. Phys. 42 (1985) 913);
S.P. Mikheyev, A.Yu. Smirnov, II Nuovo Cim. C 9 (1986) 17;
L. Wolfenstein, Phys. Rev. D 17 (1978) 2369;
L. Wolfenstein, Phys. Rev. D 20 (1979) 2634.
[17] T.K. Kuo, J. Pantaleone, Rev. Mod. Phys. 61 (1989) 937.
[18] P.I. Krastev, S.T. Petcov, Phys. Lett. B 207 (1988) 64.
[19] P.I. Krastev, S.T. Petcov, Phys. Lett. B 299 (1993) 99.
[20] P.I. Krastev, S.T. Petcov, Phys. Lett. B 285 (1992) 85.
[21] S.J. Parke, Phys. Rev. Lett. 57 (1986) 1275.
[22] S.T. Petcov, Phys. Lett. B 200 (1988) 373.
[23] Q.Y. Liu, M. Maris, S.T. Petcov, Phys. Rev. D 56 (1997) 5991. Available from <hep-ph/9702361>.
[24] S.T. Petcov, Phys. Lett. B 434 (1998) 321. Available from <hep-ph/9805262>.
[25] E.K. Akhmedov, Nucl. Phys. B 538 (1999) 25. Available from <hep-ph/9805272>.
[26] M.V. Chizhov, S.T. Petcov, Phys. Rev. Lett. 83 (1999) 1096. Available from <hep-ph/9903399>.

[27] M.V. Chizhov, S.T. Petcov, Phys. Rev. D 63 (2001) 073003. Available from <hep-ph/9903424>.
[28] J.N. Bahcall. Available from <http://www.sns.ias.edu/~jnb/>.
[29] A. Friedland, Phys. Rev. Lett. 85 (2000) 936. Available from <hep-ph/0002063>.
[30] G.L. Fogli, E. Lisi, D. Montanino, A Palazzo, Phys. Rev. D 62 (2000) 113004. Available from <hep-ph/0005261>.
[31] G.L. Fogli, E. Lisi, Astropart. Phys. 3 (1995) 185.
[32] G.L. Fogli, E. Lisi, D. Montanino, A. Palazzo, Phys. Rev. D 62 (2000) 013002. Available from <hep-ph/9912231>.
[33] M.V. Garzelli, C. Giunti, Phys. Rev. Lett. B 488 (2000) 339. Available from <hep-ph/0006026>.
[34] W.T. Eadie, D. Drijard, F.E. James, M. Roos, B. Sadoulet, Statistical Methods in Experimental Physics, North Holland, Amsterdam, 1971.
[35] A.G. Frodesen, O. Skjeggestad, H. Tofte, Probability and Statistics in Particle Physics, Universitetsforlaget, Bergen, Norway, 1979.
[36] W.H. Press, S.A. Teukolsky, W.T. Vetterling, B.P. Flannery, Numerical Recipes in C, second ed., Cambridge University Press, Cambridge, 1992.
[37] J.N. Bahcall, P.I. Krastev, A.Y. Smirnov, Phys. Rev. D 58 (1998) 096016. Available from <hep-ph/9807216>.
[38] A. Stuart, J.K. Ord, Kendall's Advanced Theory of Statistics, Vol. 1. Distribution Theory, sixth ed., Halsted Press, 1994.
[39] J. Neyman, Philos. Trans. R. Soc. Lon. Sect. A 236 (1937) 333, A selection of Early Statistical Papers on J. Neyman, University of California, Berkeley, 1967, p. 250.
[40] A. Stuart, J.K. Ord, S. Arnold, Kendall's Advanced Theory of Statistics, Vol. 2A. Classical Inference and the Linear Model, sixth ed., Oxford University Press, Oxford, 1999.
[41] C. Caso et al., Eur. Phys. J. C 3 (1998) 1.
[42] R.D. Cousins, Am. J. Phys. 63 (1995) 398.
[43] G.J. Feldman, R.D. Cousins, Phys. Rev. D 57 (1998) 3873. Available from <physics/9711021>.
[44] C. Giunti, Phys. Rev. D 59 (1999) 113009. Available from <hep-ex/9901015>.
[45] C. Giunti, M. Laveder. hep-ex/0002020.
[46] C. Guinti. hep-ex/0002042, Workshop on Confidence Limits, CERN, 17–18 January, 2000.
[47] J. Boger et al., nucl-ex/9910016.
[48] BOREXINO, F. von Feilitzsch, Prog. Part. Nucl. Phys. 40 (1998) 123.
[49] GALLEX and GNO, T.A Kirsten, Nucl. Phys. Proc. Suppl. 77 (1999) 26.
[50] F. von Feilitzsch, Neutrino 2000, Sudbury, Canada, June, 2000. http://nu2000.sno.laurentian.ca.